Synthesis and Characterization Functionalized Magnetic Nanoparticles for Biomedical Applications

Li-Fang Wang, Ying-Zhen Su, Guo-Jing Chen, Yu-Lun Lo, and Jyun-Han Ke

Department of Medicinal & Applied Chemistry, Kaohsiung Medical University, Kaohsiung 80708,
Tel: 886-7-312-1101 ext. 2217; E-mail: lfwang@kmu.edu.tw

ABSTRACT

In this study, Pluronic® F127 (PF127) modified water-dispersible superparamagnetic iron oxide nanoparticles (SPIONs), PF127-PAAIO, was prepared to prevent the recognition from the reticuloendothelial system (RES). A blood-brain-barrier (BBB) penetrating peptide, angiopep-2, was further conjugated to the surface of PF127-PAAIO (ANG-PF127-PAAIO). Their particle diameters and distributions were measured using dynamic light scattering (DLS) and a transmission electron microscope (TEM). FT-IR was used to confirm the successful synthesis of PF127-PAAIO. The cellular viabilities of U87 cells treated with both magnetic nanoparticles (MNP) were > 90%, indicating that they were non-toxic. The cellular internalization of MNPs in U87 cells were acquired using a flow cytometer and visualized using a confocal laser scanning microscope (CLSM). In conclusion, ANG-PF127-PAAIO has the ability to target the tumor section of the brain. It is potential to be used as a diagnostic imaging agent as well as a chemotherapeutic agent specifically for brain diseases.

Keywords: *Magnetic resonance imaging, PF127, Blood-brain barrier, Angiopep-2,*

1 INTRODUCTION

Magnetic resonance imaging (MRI) is an important tool for in vivo imaging diagnosis because of its harmless to human body and 3D images/soft tissue imaging ability. SPIONs having low toxicity in vivo, great biocompatibility, and outstanding superparamagnetism, are a good candidate for MRI contrast agents. Recently, SPIONs have been used in a wide range of biomedical applications such as MRI, purification/separation applications, drug delivery targeting and diagnosis, immunoassay, and hyperthermia treatment. The surface modification allows SPIONs to be more homogenous and overcome hydrophobic and toxic surface characteristics.

Pluronic® is a block copolymer containing ethylene oxide (PEO) and the propylene oxide (PPO). The hydrophilic PEO domain provides an antifouling character to prevent aggregation, protein adsorption, and recognition by the RES.[1] The hydrophobic PPO domain can be adapted to encapsulate the hydrophobic anticancer agents.

Blood-brain barrier (BBB) is a most important challenge to treat brain tumor. Different receptors on the BBB such as transferrin receptor, insulin receptor, and low-density lipoprotein receptor-related protein (LRP), play important roles in maintaining the integrity of the BBB and brain homeostasis. Angiopep-2 is a ligand of low density LRP over-expressed in human glioma cells, and possesses a high brain penetration capability of the BBB.

2 EXPERIMENT SECTIONS

2.1 Synthesis and Characterizations of PAAIO, PF127- PAAIO and ANG-PF127-PAAIO

PAAIO was synthesized using an one-step hydrolysis reaction of $FeCl_3$ at high temperature in the presence of a low molecular weight capping agent, poly(acrylic acid) (PAA) according to our previous publications.[2] PF127-succinic anhydride (PF127-Succ) was prepared by ring-opening copolymeration of succinic anhydride on PF127. PF127-PAAIO was synthesized via N-(3-dimethyl aminopropyl)-3-ethyl-carbodiimide hydrochloride (EDAC) mediated ester formation between PF127-Succ and PAAIO. ANG-PF127-PAAIO was synthesized via EDAC between Succ-PF127-PAAIO and angioepe-2. The diameters and distributions of PAAIO, PF127-PAAIO and ANG-PF127-PAAIO were measured using DLS and the morphology of MNPs was obtained from TEM. FT-IR was used to confirm the successful synthesis of PF127-PAAIO. The crystal structure of PAAIO was measured by X-ray. The magnetic properties were measured using a superconducting quantum interference device (SQUID) and T2-weighed images were generated using a magnetic resonance (MR) spectroscope equipped with a 7 T MR scanner. The composition of PAAIO, PF127-PAAIO, and ANG-PF127-PAAIO were determined using an elemental analyzer (EA)

2.2 Cell culture

U87 cells (human glioblastoma cell line) were chosen for cell culture assay. Cytotoxicities were evaluated by determining the cell viability after 24 h incubation with the MNPs using a tetrazolium-based colorimetric method (MTT conversion test). The internalized PF127-PAAIO and

ANG-PF127-PAAIO nanoparticles within U87 cells were directly visualized using Prussian blue staining of iron. The internalized amount within U87 cells was determined with a flow cytometer and the internalization mechanism was visualized directly with a confocal laser scanning microscope (CLSM) using the Rh-123-conjugated MNPs. The MRI contrast ability of MNPs in the cells was determined from the T2-weighed images. The internalized iron amount of MNPs was quantified using an inductively coupled plasma-optical emission spectrometer (ICP-OES)

3 RESULTS

The X-ray diffraction pattern of PAAIO appeared at 2θ of 30.2, 35.5, 43.2, 53.3, 57.1, and 62.8° (Figure 1), which is the same as Fe_3O_4 listed on the ASTM XRD standard card (19-0629). The characteristic peak of the ester bond stretching at 1722 cm^{-1} in Succ-PF127-PAAIO (Figure 2) implied the successful synthesis of Succ-PF127-PAAIO. The average hydrodynamic diameters of PAAIO, PF127-PAAIO and ANG-PF127-PAAIO in DD water (1 mg/mL) were 46.50 ± 1.4, 127.6 ± 29.1 and 186.5 ± 6.8 nm, respectively. The modification of PF127 and angiopep-2 on the surface of PAAIO induced an aggregation of particles. The increase in zeta-potential value from -54.30 for PAAIO to -15.90 mV for PF127-PAAIO, implied the successful conjugation of PF127 and PAAIO. The decrease in zeta-potential value from -15.90 for PF127-PAAIO to -24.30 mV for ANG-PF127-PAAIO, also implied the successful modification of angiopep-2 on PF127-PAAIO.[3] The micellar structures of PF127-PAAIO and ANG-PF127-PAAIO observed in TEM images (Figure 3), indicating that the iron oxide particles were homogeneously encapsulated inside the micelles. Based on elemental analysis measurements, the angiopep-2 content in ANG-PF127-PAAIO was ~2.72 wt%.

The saturation magnetization (σs) values of MNPs were determined using SQUID, and normalized to the Fe amount measured using ICP-OES. The σs values were 86, 80 and 76 emu/g Fe for PAAIO, PF127-PAAIO and ANG-PF127-PAAIO, respectively (Figure 4). The MNPs were superparamagnetic at room temperature and showed negligible hysteresis. The transversal relaxivities (r2) of MNPs in DD water were determined using a 7T MR scanner. The signal contrast-enhancement effect of T2-weighted MR images of PAAIO, PF127-PAAIO and ANG-PF127-PAAIO in the concentration gradient ranging from 5 to 30 mg/L iron concentration in DD water was shown in Figure 5. Transversal relaxation rates (1/T2) were plotted as a function of iron concentration, and the transversal relaxivities (r2) values obtained from the slope fitting were 178.70, 173.12 and 167.54 mM^{-1} s^{-1} for PAAIO, PF127-PAAIO and ANG-PF127-PAAIO (Figure 5). These high r2 values implied that the MNPs could be a good MRI contrast agent.

The viabilities of U87 cells exposed to the MNPs were higher than 90% at a high concentration of 500 μg/mL (Figure 6). Cytotoxicity was lower when the Fe3O4 surface was coated with PF127 and angiopep-2. The flow cytometric analysis was used to study the cellular uptake efficacy of MNPs with or without angiopep-2 moiety in U87 cells. Figure 7 shows a negligible fluorescent shift relative to the controlled group in Rh123-PF127-PAAIO, while a distinguishable right shift was observed in Rh123-ANG-PF127-PAAIO, indicating a better cellular uptake even at a low MNPs concentration of 100 μg/mL and at an incubation time for 30 min. The increased cellular uptake into U87 cells of MNPs with an angiopep-2 moiety was significant as compared to without when the incubation time was extended to 2 h. The internalization of MNPs in U87 cells was directly stained with Prussian blue. The internalized Fe^{3+} ions of MNPs turned to bright blue pigment when reacting with the ferrocyanide ions. This blue color was visualized using an optical microscope. There was no discernible blue color in U87 cells after 30 mins or 2 h incubated with PF127-PAAIO. In contrast, clearly blue color was observed after 30 mins and became more noticeable after 2 h, as the cells were incubated with ANG-PF127-PAAIO. The cellular uptake of MNPs in U87 cells was quantified by measuring the iron content per cell using ICP-OES (Figure 9). The mean data of the cellular iron contents in U87 cells were 5.2 and 8.1 μg Fe/mg protein for PF127-PAAIO and ANG-PF127-PAAIO after 30 min of incubation, and 6.0 and 10.2 μg Fe/mg protein after 2 h of incubation. This result was in a good agreement with the finding using flow cytometry, where ANG-PF127-PAAIO clearly had the better cellular uptake in U87 cells. As compared the confocal image with Rh123-PF127-PAAIO, the Rh123-ANG-PF127-PAAIO showed higher fluorescence intensities after 2 h of incubation (Figure 10). The potential of MNPs as a targeted MR contrast agent to cancer cells was determined from the *T*2-weighted MR phantom images. The rapid and efficient angiopep-2 receptor-mediated endocytosis led to a distinguishable darkening of MR images of the cells incubated with ANG-PF127-PAAIO as compared with PF127-PAAIO at a Fe concentration of 30 μg/mL.

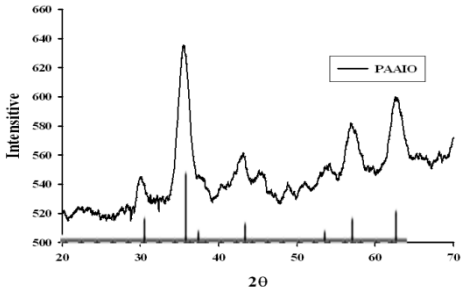

Figure 1. X-ray diffraction patterns for PAAIO nanoparticles.

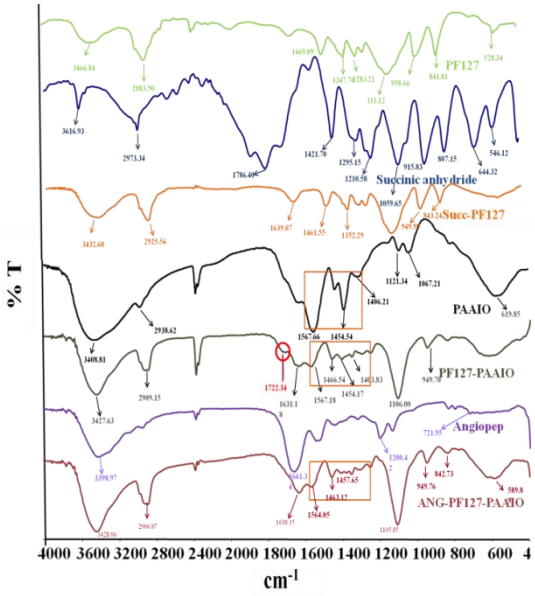

Figure 2. FTIR spectrum of PF127, succinic anhydride. Succ-PF127, PAAIO, Aniopep-2, ANG-PF127-PAAIO.

Table 1. The hydrodynamic diameter and size distribution of PAAIO, PF127-PAAIO and ANG-PF127-PAAIO (n= 3).

	D_h (nm)	PDI	V (mV)
PAAIO	46.5 ± 1.4	0.27 ± 0.10	-54.30 ± 0.28
PF127-PAAIO	127.6 ±29.1	0.26 ± 0.05	-15.90 ± 2.73
ANG-PF127-PAAIO	186.5 ± 6.8	0.32 ± 0.06	-24.30 ± 3.46

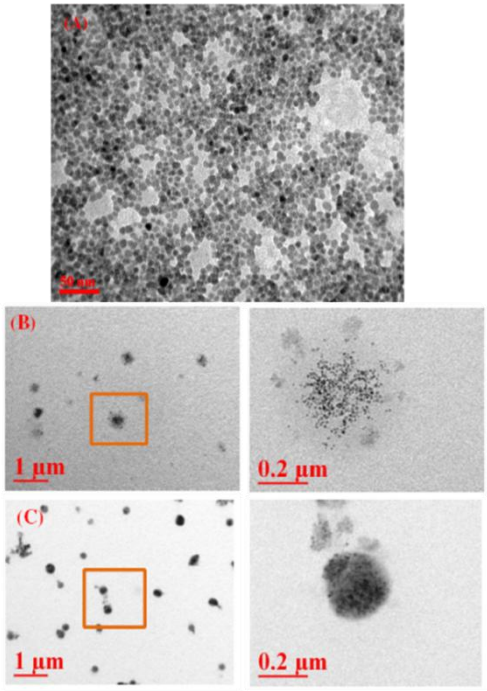

Figure 3. Transmission electron microscope (TEM) images of (A) PAAIO; (B) PF127-PAAIO; (C) ANG-PF127-PAAIO.

Table 2. The composition of PAAIO, PF127-PAAIO and ANG-PF127-PAAIO (n= 3).

	PAAIO (wt %)	PF127* (wt %)	Angiopep-2* (wt %)
PAAIO	100	-	-
PF127-PAAIO	41.70 ± 2.15*	58.30 ± 2.15	-
ANG-PF127-PAAIO	40.64 ± 1.21	56.47 ± 1.21	2.72 ± 0.01

*Determined by elemental analyzer (EA)

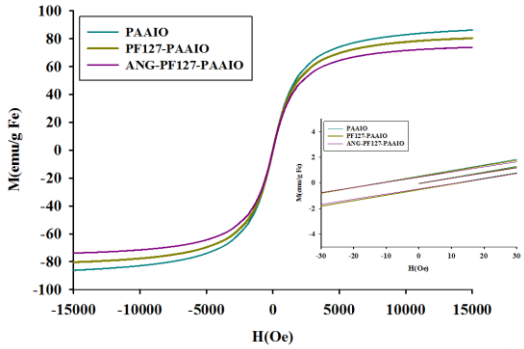

Figure 4. The magnetization curve as a function of field for PAAIO, PF127-PAAIO and ANG-PF127-PAAIO.

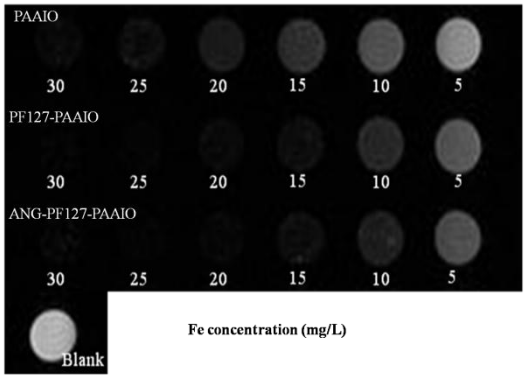

Figure 5. T2-weighted magnetic resonance (MR) phantom images for PAAIO, PF127-PAAIO and ANG-PF127-PAAIO.

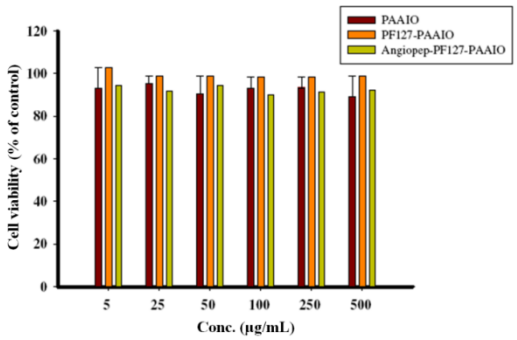

Figure 6. The viability of U87 cells exposed to PAAIO, PF127-PAAIO and ANG-PF127-PAAIO after 24 h of incubation. (n= 3)

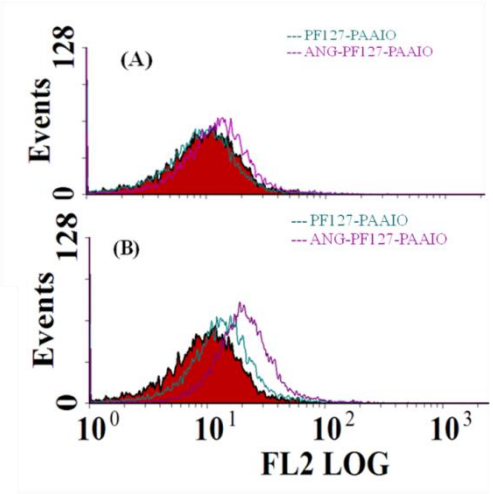

Figure 7. Flow cytometric diagrams of PF127-PAAIO-Rh123 and ANG-PF127-PAAIO-Rh123 in U87 cells after 30 min (A) and 2h (B) of incubation.

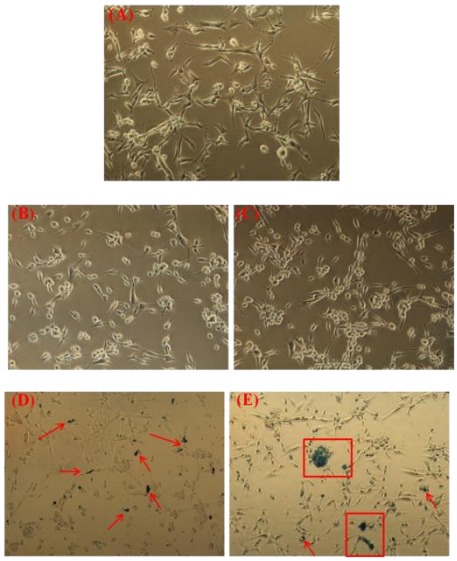

Figure 8. Prussian blue-stained U87 cell after incubation without (A) or with the PF127-PAAIO (B, C) and ANG-PF127-PAAIO (D, E) for 30 min (B, D) or 2 h (C, E) at 37 °C.

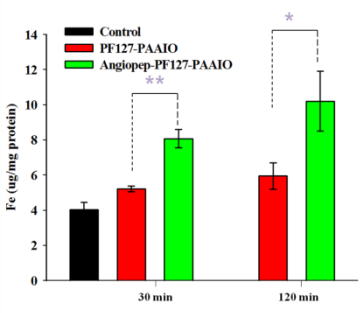

Figure 9. The iron content in U87 cells due to the uptake of PF127-PAAIO and ANG-PF127-PAAIO.

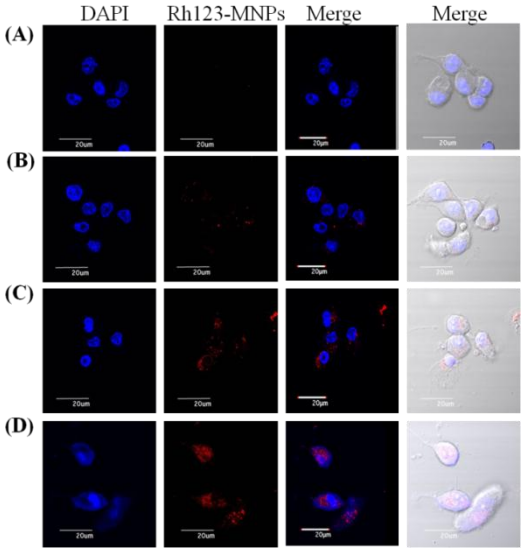

Figure 10. CLSM images of U87 cells exposed to PF127-PAAIO-Rh123 (A, B) and ANG-PF127-PAAIO- Rh123 (C, D) for 30 min (A, C) and 2 h (B, D) at 37 ℃.

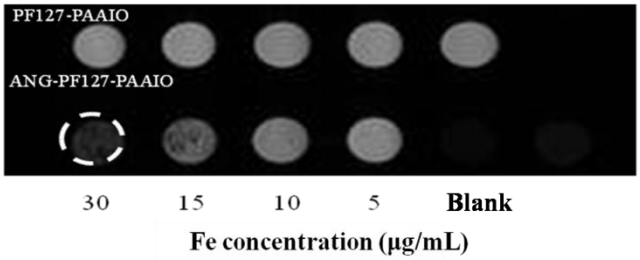

Figure 11. *T*2-weighted MR phantom images of U87 cells after incubation with the various concentrations of PF127-PAAIO and ANG-PF127-PAAIO.

4 SUMMARY

We successfully synthesized brain tumor targeting magnetic nanoparticles, ANG-PF127-PAAIO. The BBB penetrating peptide indeed enhanced ANG-PF127-PAAIO to enter the U87 cells. Thus, Angiopep-PF127-PAAIO is potential to be used as a diagnostic imaging agent as well as a chemotherapeutic agent specifically for treatment of brain diseases.

REFERENCES

[1] M. Garinot, V. Fievez, V. Pourcelle, F. Stoffelbach, A. des Rieux, L. Plapied, I. Theate, H. Freichels, C. Jerome, J. Marchand-Brynaert, Y. J. Schneider, V. Preat, *J Control Release* **2007**, *120*, 195.
[2] J. J. Lin, J. S. Chen, S. J. Huang, J. H. Ko, Y. M. Wang, T. L. Chen, L. F. Wang, *Biomaterials* **2009**, *30*, 5114.
[3] H. H. Yan, J. Y. Wang, P. W. Yi, H. Lei, C. Y. Zhan, C. Xie, L. L. Feng, J. Qian, J. H. Zhu, W. Y. Lu, C. Li, *Chem Commun* **2011**, *47*, 8130.